System-based probabilistic optimization of fluid viscous dampers equipped in cable-stayed bridges

Jian Zhong[1] , Zhangliang Hu[1], Wancheng Yuan[2] and Liang Chen[1]

Abstract

This study presents a methodology to evaluate the optimal parameters of fluid viscous damper for cable-stayed bridges using the system-level fragility assessment approach. Instead of investigating the impact of different isolation devices on the component's vulnerability separately, this study focuses on evaluating the optimal parameters of fluid viscous damper to achieve the best overall performance of cable-stayed bridge as a system. Numerical model of a cable-stayed bridge with the most common configuration in China is established using OpenSEES that can account for their nonlinear response and uncertainty treatment. A joint probabilistic seismic demand model and Monte Carlo simulation are employed to obtain the system fragility of cable-stayed bridges by accounting for the contribution of multicomponents to the global damage state. The system-level fragility curves and component fragility curves are compared before and after the application of fluid viscous damper with different parameters. The results indicate that a given parameter of the fluid viscous damper may have a negative impact on some components, yet lead to a better performance of the bridge as a system. Thus, in order to obtain comprehensive knowledge of bridge performance and derive the accurate optimal parameters of fluid viscous damper, it is necessary to consider the fragility based on bridge system.

Introduction

In recent decades, cable-stayed bridges have been widely constructed around the world because of their aesthetics, efficient use of construction materials, and fast construction period. Many studies focused on the dynamic characteristics of cable-stayed bridges subjected to earthquake (Bruneau, 1992; Ren and Obata, 1999; Wilson and Gravelle, 1991). These studies showed that the seismic demand of towers would experience a significant increase in terms of bending moment and shear forces when restraining the bridge deck completely at tower locations. When there are no additional restraints in the longitudinal direction, larger deck displacement would occur during earthquake, resulting in pounding and unseating (Aiken and Kelly, 1992), which is not desirable for performance-based earthquake engineering. Therefore, there is an agreement among many researchers that mitigation devices should be equipped to allow some sort of deck movement, which would lead to the balance of the force and displacement demand of the cable-stayed bridges (Sharabash and Andrawes, 2009). Many researchers have conducted work on the isolation

devices to reduce the overall seismic response of cable-stayed bridges (Ali and Abdel-Ghaffar, 1994; Sharabash and Andrawes, 2009; Zhang et al., 2009; Zhu and Qiu, 2014); however, these studies are determined methods, which could not account for the earthquake uncertainties, because of the unpredictable nature of seismic events (Zhang and Huo, 2009).

In order to consider the uncertainties of earthquake and structure information, it is a widely used approach to develop probabilistic model in the form of fragility curves (Basoz et al., 1999; Choi et al., 2004; Hwang et al., 2001; Nielson, 2005; Padgett and DesRoches, 2008; Pan et al., 2007; Ramanathan, 2012; Shinozuka et al., 2000a, 2000b). Fragility function is quite useful

[1]School of Civil and Hydraulic Engineering, Hefei University of Technology, Hefei, P.R. China
[2]State Key Laboratory of Disaster Reduction in Civil Engineering, Tongji University, Shanghai, P.R. China

Corresponding author:
Liang Chen, School of Civil and Hydraulic Engineering, Hefei University of Technology, Hefei 230009, P.R. China.
Email: popecl@hfut.edu.cn

for comparing and selecting mitigation strategies. Casciati et al. (2008) evaluated the seismic vulnerability of components (bending moment, shearing force, deck displacement, cable strain, etc.) of a cable-stayed bridge with passive hysteretic devices in terms of damage exceedance probability. Barnawi and Dyke (2014) developed component (deck displacement, overturning moment, deck shear, etc.) fragility curves of a benchmark cable-stayed bridge equipped with response modification systems. These studies evaluated the effectiveness of the mitigation devices using component fragility separately, rather than the system fragility of the overall bridge performance. For example, some kind of isolation devices might decrease the fragility of bending moment, but would increase the fragility of deck displacement. Hence, a comprehensive evaluation of seismic isolation on bridges should be based on system-level fragility instead of on the component level. It is still worth noting that the above-mentioned studies did not emphasize on selecting optimum mitigation devices to achieve the best performance of cable-stayed bridges.

This article will use the system fragility function method to investigate the efficiency of isolation device and derive the optimal parameters to achieve the best overall performance of cable-stayed bridges. A long-span cable-stayed bridge with the most common configuration in China is chosen and a numerical model is built using OpenSEES (McKenna and Fenves, 2010) that can account for their nonlinear response and the uncertainties in the ground motion and structural properties. This article will mainly focus on the viscous damper, which is a widely used mitigation device equipped in cable-stayed bridges. Fragility curves of bridges at system level are derived from the multi-dimensional damage model considering the correlations between the components of cable-stayed bridge. The fragility at system level of cable-stayed bridge equipped with different viscous dampers is compared. Finally the optimal parameters are derived.

Methodology for optimal design of viscous damper

This study describes the methodology of the optimization and sensitivity analysis of fluid viscous damper (FVD) based on system-level fragility functions. The flow chart is illustrated in Figure 1 and described as follows.

Step 1: establish probabilistic seismic demand model and capacity model

The fragility can be simply defined as the conditional probability that the seismic demand (D) placed upon the structure exceeds its capacity (C) for a given *IM* level, as shown in the following equation

$$Fragility = P[D>C|IM] \tag{1}$$

The demand model (S_D) is conventionally defined as a linear regression model in a log-transformed space (Cornell et al., 2002), obtained from the simulations

$$S_D = aIM^b \tag{2}$$

where a and b are regression coefficients. Practically, the fragility function can be expressed assuming that both the demand and capacity follow lognormal distributions

$$P[D \geqslant C|IM] = \Phi\left(\frac{\ln(S_D) - \ln(S_C)}{\sqrt{\beta_{D|IM}^2 + \beta_C^2}}\right) \tag{3}$$

where S_D and $\beta_{D|IM}$ are the median value and dispersion, respectively, of the demand as a function of an *IM*; S_C and β_C are the median value and dispersion, respectively, of the structural capacity; and $\Phi(\bullet)$ is the cumulative distribution function of the standard normal distribution. The dispersion of the demand model can be expressed as

$$\beta_{D|IM} = \sqrt{\frac{\sum\left[\ln(d_i) - \ln(S_D)\right]^2}{(n-2)}} \tag{4}$$

where d_i is the *i*th realization of the demands obtained from simulations and n is the number of simulations.

Limit state models reflect multiple levels of structural functionality associated with observed damage. As mentioned before, each limit state model follows a distribution with two parameters, S_C and β_C.

Step 2: correlation coefficient matrix calculation and system-level fragility deriving

The general assessment of seismic vulnerability for the bridge system as a whole must be made by combining the effects of various bridge components (Nielson and DesRoches, 2007). The multi-dimensional integral defining the seismic risk and involved in optimization cannot be calculated, or even accurately approximated, analytically. Therefore, joint probabilistic seismic demand model (JPSDM) and Monte Carlo sampling (MCS) are employed to obtain the system-level fragility by the stochastic analysis. JPSDM is developed in a log-transformed state by considering the correlation between transformed demands of various bridge components. MCS is performed in which N random samples are generated from both the JPSDM and limit
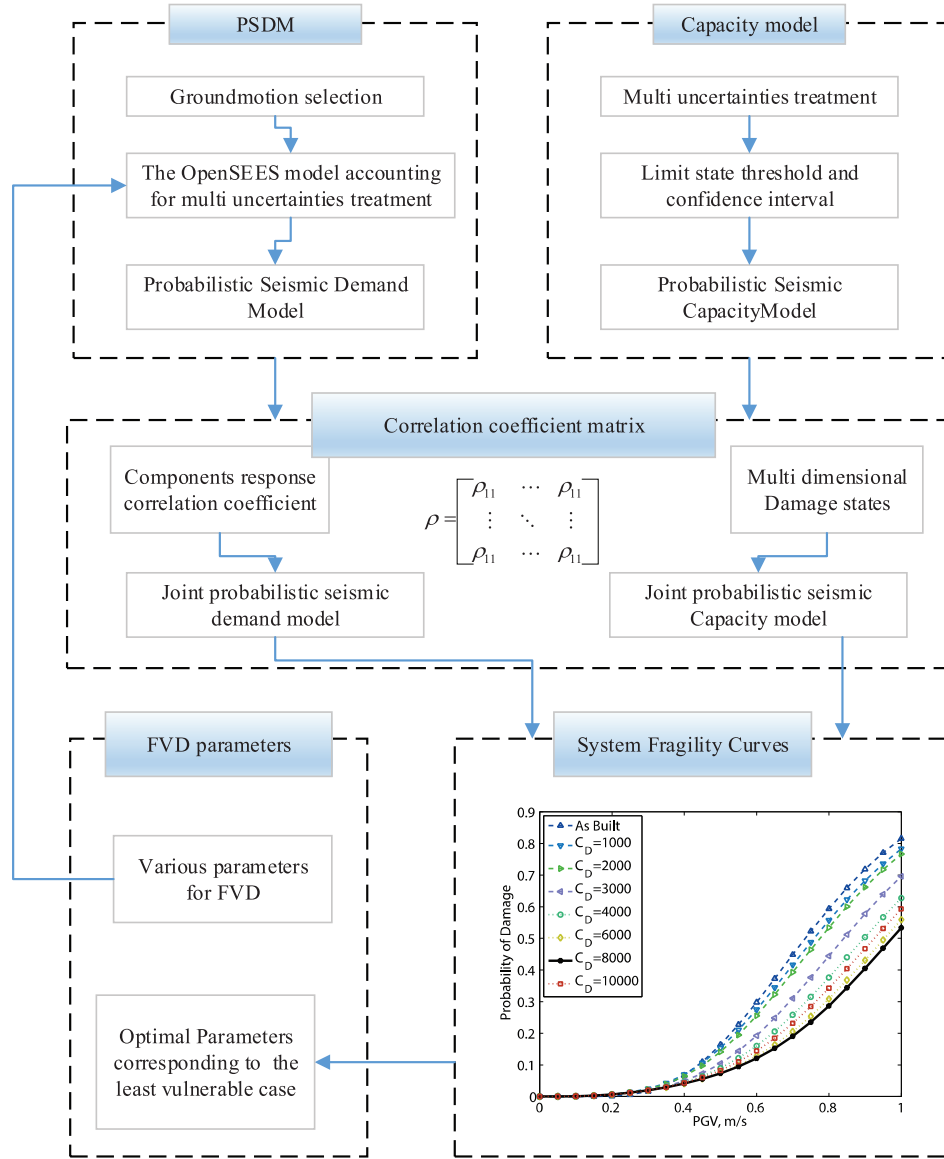
Figure 1. Flow chart for methodology of optimization and sensitivity analysis of FVD based on system-level fragility functions.

state model. Each sampling demand is evaluated in the sampling failure domain and tracked by an indicator function (I_F). The indicator function of n components is presented in equation (5)

$$I_F = \begin{cases} 1 & if \quad (x_1, x_2, ..., x_n) \in F_{1,2,...,n} \\ 0 & if \quad (x_1, x_2, ..., x_n) \notin F_{1,2,...,n} \end{cases} \quad (5)$$

where $(x_1, x_2, ..., x_n)$ is the sampling of the n components demand and, $F_{1,2,...,n}$ is the multi-dimensional failure domain defined by the limit state of various components. At a given IM, the probability of being in the failure domain is estimated as

$$P[Fr_{system}|IM = a] = \frac{\sum_{i=1}^{N} I_{F_i}}{N} \quad (6)$$

By performing the MCS from a wide range of IMs, the entire curve of the system fragility can be obtained.

Step 3: optimization and sensitivity analysis based on system-level fragility functions

The system fragility curves are the object function. Conduct the system-level fragility analysis for each cable-stayed bridge equipped with different viscous dampers. Compare the fragility function for each case and derive the minimal system fragility function, and the corresponding viscous damper parameters are the optimal one. The advantage of this approach is the ability to evaluate the impact of retrofit on multiple vulnerable components as well as the bridge's overall seismic performance.
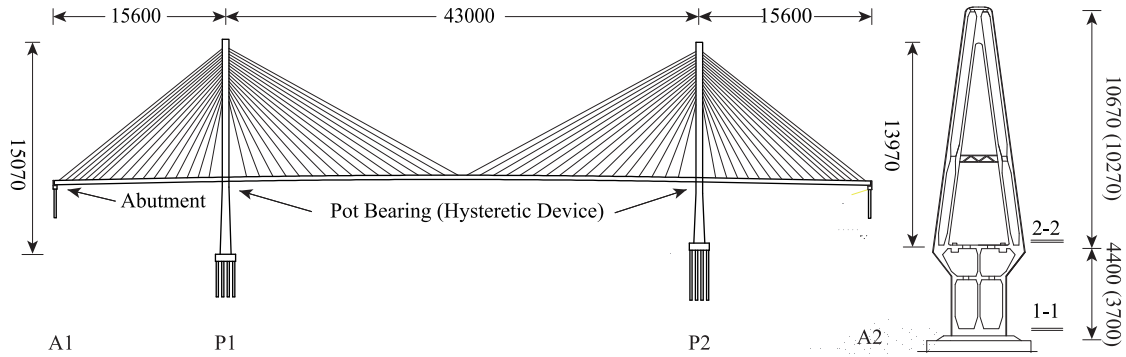
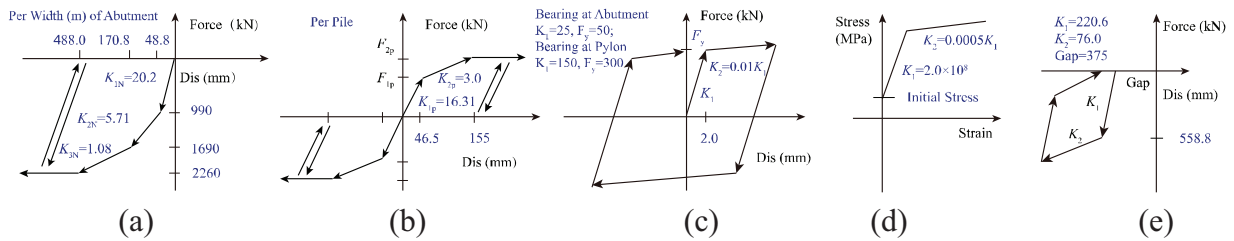**Figure 2.** Configuration of Polonggou cable-stayed bridge (unit: cm).

Figure 3. Force-deformation relations of various components: (a) abutment passive, (b) abutment active, (c) pot bearing, (d) cables, and (e) pounding.

Case study

Input ground motions

This study selects the suite of ground motions used in Shafieezadeh et al. (2012), which comprises 80 ground motions extracted from the PEER Strong Motion Database and 20 ground motions pertinent to Los Angeles selected from the SAC project database. The 80 PEER ground motions have an even selection of recorded time-histories from four bins that include combinations of low and high moment magnitudes as well as large and small epicentral distances.

Bridge description and numerical model

This study selects Polonggou Bridge, which is the most common type of cable-stayed bridge constructed in China. It has three spans; the main span and side span are 430 and 156 m, respectively. The 17 stay cables are arranged in a fan configuration. The detailed geometry of the cable-stayed bridge is shown in Figure 2.

Using the OpenSEES analysis platform (McKenna and Fenves, 2010), which is an open-source collaborative software framework for simulating the seismic response of structural and geotechnical systems, a detailed nonlinear three-dimensional model is created for the subject bridge. The superstructure is expected to remain linear and is thus modeled using elastic beam-column elements. A distributed plasticity fiber model is used to represent sections of pylons to account for the axial force-moment interaction and material nonlinearity. Foundations of the pylons are modeled using six spring elements (Zhong et al., 2016). The response of each cable is simulated using a nonlinear tension-only element, which is modeled as a large-displacement truss element using the Ernst method or modified elastic modulus method as a result of the easy usage and the capability to account for the sag effect (Pang et al., 2014). The initial stress of the cable is also considered in the model (Figure 3(d)). The abutment element comprising passive, active, and transverse actions is modeled by the stiffness of the passive resistance of the backfill soil (Figure 3(a)) and the stiffness of the piles (Figure 3(b)) (Choi et al., 2004; Nielson, 2005; Padgett and DesRoches, 2008). The pounding effect (Figure 3(e)) between the superstructure and abutment is modeled using the contact element approach developed by Muthukumar and DesRoches (2006), which includes hysteretic energy loss. The longitudinal response of the pot bearing (Figure 3(c)) is simulated using a nonlinear bilinear element, while the transverse response of the bearing is assumed to be constrained. Further details on the assumptions and analytical models themselves can be found elsewhere (Zhong et al., 2016, 2017).

Table 1. Demand parameters of different bridge components considered.

Engineering demand parameters	Abbreviation	Unit
Longitudinal curvature ductility in the Section 1 Pylon 1	$\mu_{\varphi\text{-}P1S1}$	–
Longitudinal curvature ductility in the Section 2 Pylon 1	$\mu_{\varphi\text{-}P1S2}$	–
Longitudinal curvature ductility in the Section 1 Pylon 2	$\mu_{\varphi\text{-}P2S1}$	–
Longitudinal curvature ductility in the Section 2 Pylon 2	$\mu_{\varphi\text{-}P2S2}$	–
Abutment passive displacement	δ_{AP}	mm
Abutment active displacement	δ_{AA}	mm
Pot bearing displacement at Pylon 1	δ_{PB}	mm
Relative displacement of abutment and deck	δ_{AD}	mm

Table 2. Demand models and regression parameters.

EDP	b	β	ζ
$\mu_{\varphi\text{-}p1s1}$	0.896	0.310	0.346
$\mu_{\varphi\text{-}p1s2}$	0.754	0.230	0.305
$\mu_{\varphi\text{-}p2s1}$	1.539	0.830	0.539
$\mu_{\varphi\text{-}p2s2}$	1.348	1.210	0.898
δ_{AP}	1.296	0.570	0.440
δ_{AA}	0.728	0.500	0.687
δ_{PB}	1.012	0.480	0.474
δ_{AD}	1.011	0.450	0.445

EDP: engineering demand parameter.

Engineering demand parameters

Demands placed on critical components are taken into account for the vulnerability assessment of bridges. In this study, peak demands of components are adopted as engineering demand parameters (EDPs), and the critical components are the pylons, bearings, abutments, and the relative displacement of abutment and deck, as listed in Table 1.

Probabilistic seismic demand model

Selecting an optimal IM for seismic fragility assessment is not a trivial matter and has been focused on in numerous studies (Padgett et al., 2008, Shafieezadeh et al., 2012). In some of the pioneering works, various IMs were selected as optimal IM, including Modified Mercalli Intensity Scale (ATC, 1985), peak ground acceleration (PGA) (FEMA 1997), peak ground displacement (PGD), spectral acceleration at a period of 1 s (Ramanathan, 2012), and vector-based IMs (Baker and Cornell, 2005; Luco and Cornell, 2007). However, for long-period structures, especially for long-span cable-stayed bridges, peak ground velocity (PGV) was demonstrated to be the optimal IM (Zhong et al., 2016). Therefore, PGV is chosen as the intensive measure in this study. The linear fit parameters and the dispersion in the log-log space are shown in Table 2.

## Components classification and limit states definition

This study partially employs existing models or definitions of limit states used in previous studies. The limit states for the abutments follow the work of Ramanathan (2012). The design displacement of the pot bearing is ±300 mm. Thus, two limit states are defined for the pot bearing; LS1 is 300 mm and LS2 is 600 mm. Limit states for the abutment seat is intimately linked to the unseating of superstructure. This study uses the moderate (LS2) and extensive (LS3) limit states for the abutment seat determined per the definition of Avşar et al. (2011), which is illustrated in Table 3. The LS3 and LS4 of the abutment and bearing are not defined because these components are regarded as accessory components and thus contribute only to the slight and moderate damage of cable-stayed bridges.

The column is the most critical component of bridges when performing the fragility analysis of bridges. Several previous studies (Nielson and DesRoches, 2007; Pan et al., 2007; Ramanathan, 2012; Zhang and Huo, 2009) defined different limit states for columns and achieved different conclusions. However, the limit states are related to the geometry of the section, material, and volumetric percentage of the confining steel, and axial compression ratio of the section. Thus, numerical simulation is employed to derive the

Table 3. Limit state models for various EDPs.

EDPs	LS1		LS2		LS3		LS4	
	S_C	β_C	S_C	β_C	S_C	β_C	S_C	β_C
$\mu_{\varphi\text{-}p1s1}$	1.00	0.35	1.33	0.35	4.52	0.35	24.8	0.35
$\mu_{\varphi\text{-}p1s2}$	1.00	0.35	–	–	1.37	0.35	6.27	0.35
$\mu_{\varphi\text{-}p2s1}$	1.00	0.35	1.33	0.35	4.52	0.35	24.8	0.35
$\mu_{\varphi\text{-}p2s2}$	1.00	0.35	–	–	1.37	0.35	6.27	0.35
δ_{AP}	48.8	0.35	170.8	0.35	–	–	–	–
δ_{AA}	46.5	0.35	155.0	0.35	–	–	–	–
δ_{PB}	300	0.10	600	0.10	–		–	–
δ_{AD}	–	–	1980	0.10	2625	0.10	–	–

EDPs: engineering demand parameters.
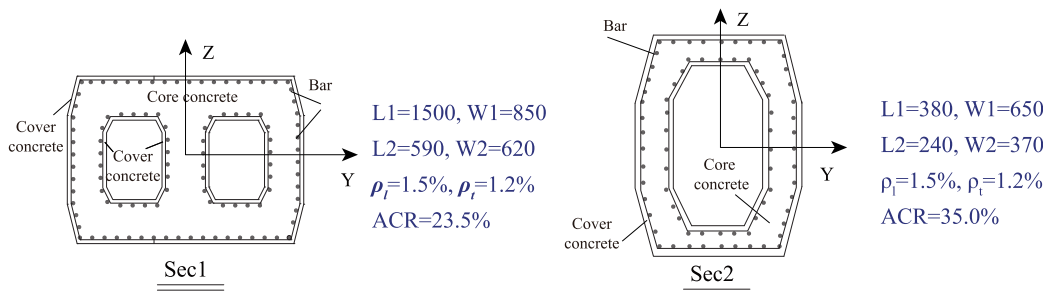
Figure 4. Fiber section of sections 1 and 2.

limit states of the pylon sections. First, a fiber section is created using OpenSEES (McKenna and Fenves, 2010), as shown in Figure 4, and a pushover analysis is then performed to obtain the moment-curvature curve of the sections. The normalized values of the curvature with respect to φ_1 are listed in Table 3.

Component and system-level fragility curves

Using the probabilistic seismic demand model (PSDM) and the limit states in the framework of equation (3), fragility curves for each of bridge components are easily calculated and plotted in Figure 5. The pot bearing (δ_{PB}) appears to be the most vulnerable component at the slight damage state, followed by the abutments (δ_{AP} and δ_{AA}). For the moderate damage state, the pot bearing (δ_{PB}) is still the most vulnerable component, but followed by section 1 of pylon 2 ($\mu_{\varphi\text{-}p2s1}$). However, section 1 of pylon 2 ($\mu_{\varphi\text{-}p2s1}$) are the most vulnerable components at the extensive damage state and complete damage state, respectively. For all the damage states, pylon 2 is more vulnerable than pylon 1. This is associated with the fact that pylon 1 is longer and more flexible than pylon 2, and thus pylon 2 experiences larger seismic demands than pylon 1.

$X = (X_1, X_2, ..., X_{12})$ represents the vector of demands, placed on the EDPs of the cable-stayed bridge, and $Y = \ln(X)$ is the vector of demands in the log-transformed space. JPSDM is then formulated in the log-transformed space by assembling the vector of means $\mu_Y(PGV = pgv)$ and the covariance matrix σ_Y. The correlation coefficient matrix of the demand of 8 EDPs is listed in Table 4. MCS is used to compare realizations of the demand and capacity of components to calculate the failure probability of the system using equation (6). Finally, a system fragility curve can be determined as a lognormal cumulative distribution function with two parameters (median and dispersion) by performing a regression analysis, which is shown in Figure 5.

Optimization of FVD based on system fragility function

Polonggou cable-stayed bridge is located in the border of Sichuan and Tibet of China, which is prone to experience large earthquake. Viscous fluid dampers, deemed as passive energy dissipation devices for seismic protection of structures, are equipped in the cable-stayed bridge which possess lower damper, as shown in Figure 6.

Experimental testing has shown that a suitable mathematical model for describing the behavior of
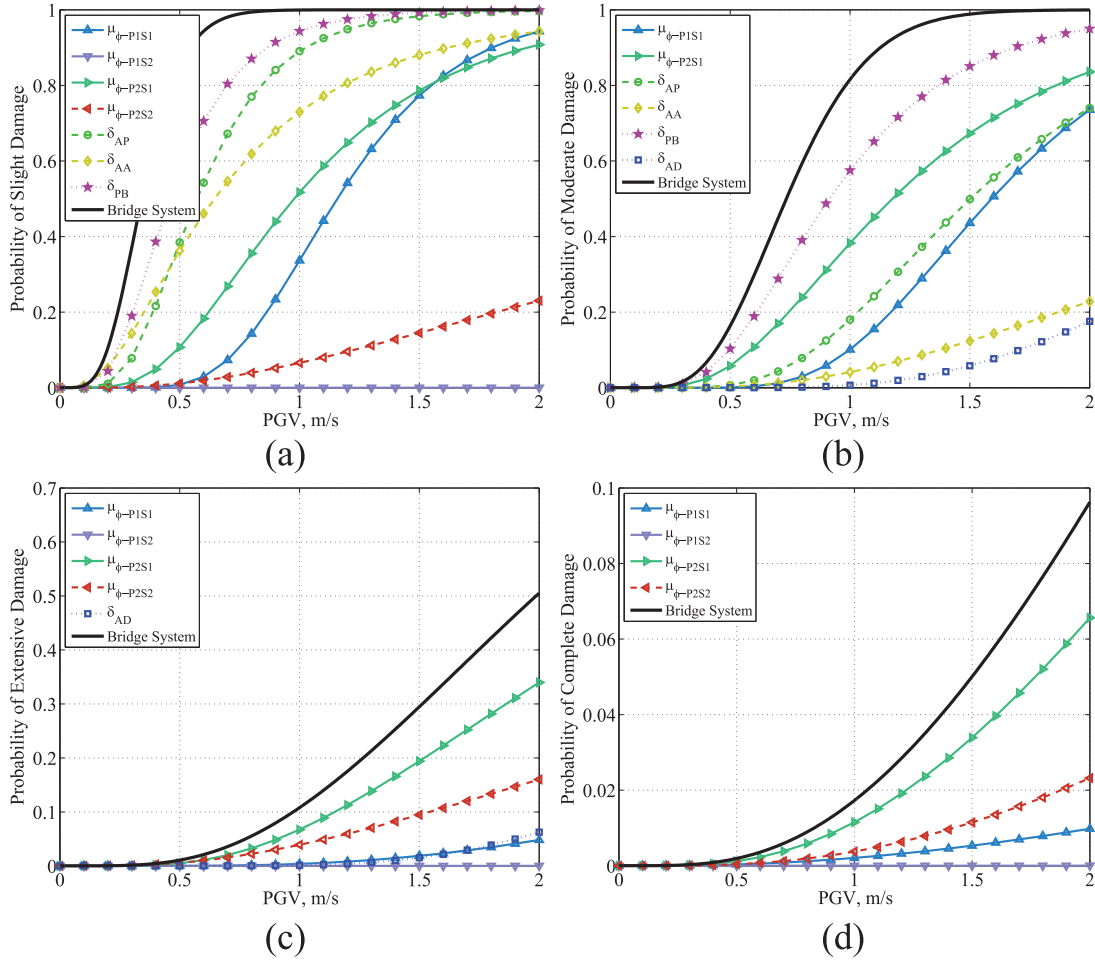
Figure 5. Component and system fragility curves for the cable-stayed bridge: (a) slight damage, (b) moderate damage, (c) extensive damage, and (d) complete damage.

Table 4. Correlation coefficients between transformed demands.

	$\mu_{\varphi\text{-}P1S1}$	$\mu_{\varphi\text{-}P1S2}$	$\mu_{\varphi\text{-}P2S1}$	$\mu_{\varphi\text{-}P2S2}$	δ_{AP}	δ_{AA}	δ_{PB}	δ_{AD}
$\mu_{\varphi\text{-}P1S1}$	1.000	0.722	0.589	0.471	0.656	0.327	0.665	0.698
$\mu_{\varphi\text{-}P1S2}$	0.722	1.000	0.347	0.512	0.766	0.136	0.841	0.842
$\mu_{\varphi\text{-}P2S1}$	0.589	0.347	1.000	0.179	0.370	0.380	0.436	0.468
$\mu_{\varphi\text{-}P2S2}$	0.471	0.512	0.179	1.000	0.438	0.203	0.539	0.535
δ_{AP}	0.656	0.766	0.370	0.438	1.000	0.194	0.759	0.764
δ_{AA}	0.327	0.136	0.380	0.203	0.194	1.000	0.045	0.049
δ_{PB}	0.665	0.841	0.436	0.539	0.759	0.045	1.000	0.992
δ_{AD}	0.698	0.842	0.468	0.535	0.764	0.049	0.992	1.000

viscous fluid dampers is given by the following non-linear force–velocity relation
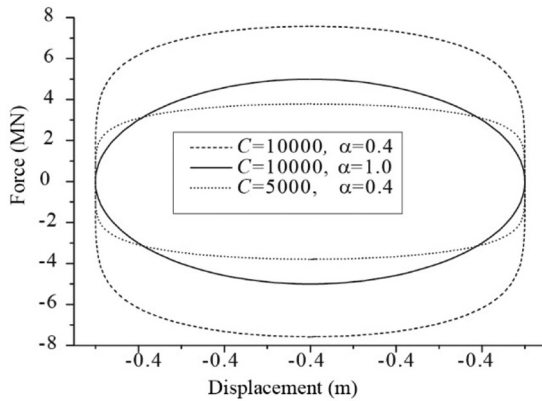
$$f_D = C_D |\dot{u}|^{\alpha} \text{sgn}(\dot{u}) \qquad (7)$$

where f_D is the force developed by the damper; u is displacement across the damper; α is a real positive exponent whose value is determined by the piston head orifice design; C_D denotes the damping coefficient with units of force per velocity raised to the power α; sgn(·) is the signum function; and the over dot indicates differentiation with respect to time, t. The exponent α typically has a value usually ranging from about 0.2 to 0.4 for cable-stayed bridges, 0.3 is selected in this study

Figure 6. The Polonggou Bridge during construction and the application of FVD.


Figure 7. The restore curves of FVD.

δ_{PB}. Note that higher median PGV in Figure 9 indicates less vulnerability of the given component.

The optimal parameters of FVD varied when focused on different components. Hence, the importance of characterizing not only the component vulnerability but also system-level impact of FVD is emphasized. The component fragility curves analysis leads to a need to evaluate the comprehensive insight of the overall system vulnerability of the cable-stayed bridge. The system fragility curves are developed by considering the contribution of multiple vulnerable components. Increasing the C_D from 3.0×10^3 to 8.0×10^3 would have a negative impact on pylon 1 (increasing the fragility of $\mu_{\varphi\text{-}P1S1}$), yet lead to a better performance of the cable-stayed bridge as a system (reducing the system-level fragility). Consideration of the fragility based only on individual retrofitted components, without regard for the system, may lead to over-estimation or under-estimation of the impact on the bridge fragility. The importance of developing system-level retrofitted bridge fragility curves is again recognized. For example, changing the C_D from 8.0×10^3 to 1.0×10^4 would have reduced vulnerability of unseating, but would increase the probability of damage as a bridge system. As shown in Figure 10, as a system, the Polonggou cable-stayed bridge tends to be less vulnerable when C_D varies from 1.0×10^3 to 8.0×10^3 and turns more vulnerable when the C_D becomes larger than 8.0×10^3. Thus, we can make a conclusion that the optimal parameter of FVD is 8.0×10^3 to achieve the best performance of Polonggou cable-stayed bridge subjected to earthquake.

for α, and investigates the optimal C_D for Polonggou cable-stayed bridge (Figure 7).

Parametric study and optimization of dampers are performed with the exponent α as 0.3 and the damping coefficient of the viscous dampers C_D varying from 1.0×10^3 to 10×10^3.

The component fragility curves are compared before and after the application of FVD with different parameters, as illustrated in Figure 8. The results indicate that increasing the additional damper of the cable-stayed bridge could reduce displacement of the bridge, resulting in reducing the probability of damage of displacement related EDPs (the bearing, the abutment, the unseating, etc.) for a given intensity measure. So the optimal C_D is 1.0×10^4 in terms of the bearing abutment and unseating performance. Changing the C_D from 1.0×10^3 to 1.0×10^4 would increase the seismic force of the bridge, but the bending moment would not increase until C_D is larger than 3.0×10^3 and 1.0×10^4 for pylon 1 and pylon 2, respectively. The optimal C_D is 3.0×10^4 or 8.0×10^4 if we focus only on the vulnerability based on pylon 1 or pylon 2. The trends are evident and are shown clearly in Figure 9 which depicts the median value of fragility curves of $\mu_{\varphi\text{-}P1S1}$, $\mu_{\varphi\text{-}P2S1}$, and

Conclusion

Seismic retrofit measures tend to focus on individual component response, less research has been carried out on the cable-stayed bridge performance as a system, and the optimal parameters of retrofit devices have not been addressed in the literature. This study presents a
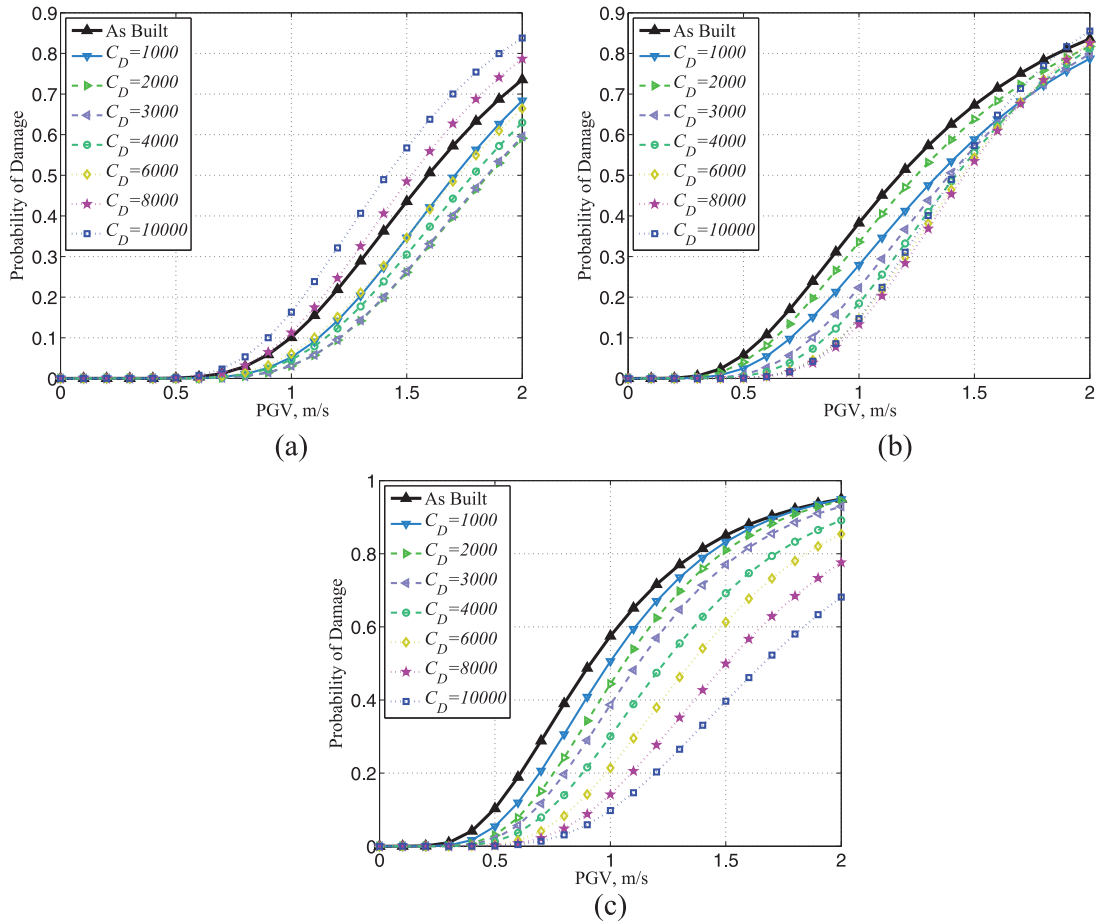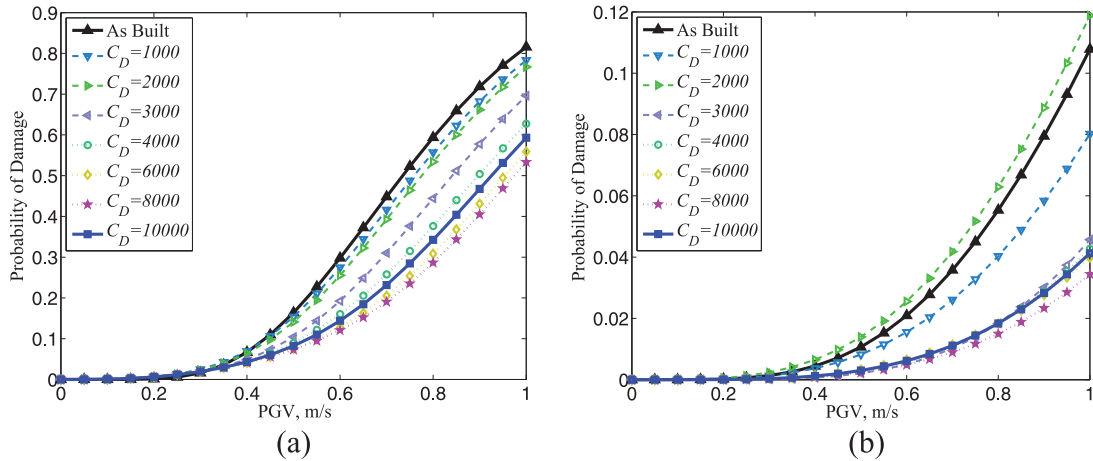
Figure 8. Moderate fragility curves of components of Polonggou cable-stayed bridge equipped with varied FVD: (a) $\mu_{\varphi\text{-}P1S1}$, (b) $\mu_{\varphi\text{-}P2S1}$, and (c) δ_{PB}.
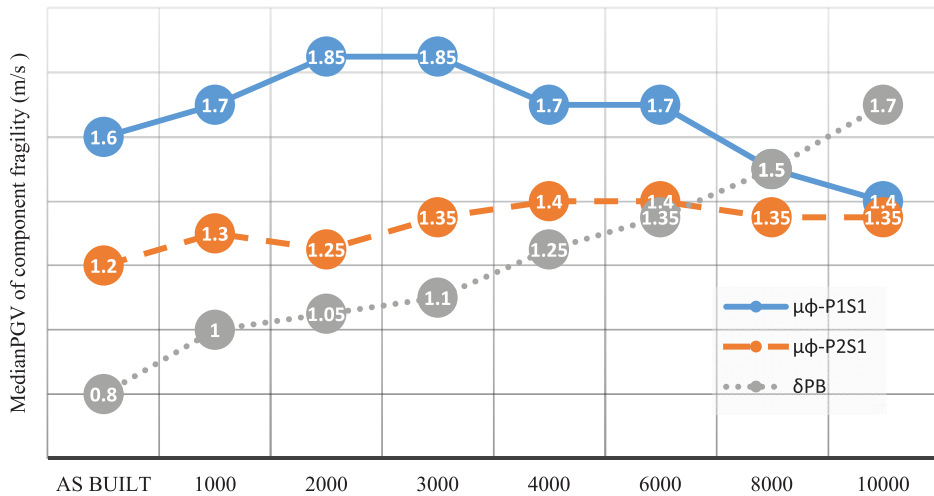
Figure 9. The median value of fragility of each component.

methodology to evaluate the optimal parameters of FVD for cable-stayed bridges using the system-level fragility function. JPSDM and Monte Carlo simulation are employed to obtain the system fragility of cable-stayed bridges by accounting for the contribution of multi components to the global damage state. Optimal

Figure 10. System-level fragility curves of Polonggou cable-stayed bridge equipped with varied FVD: (a) moderate damage and (b) extensive damage.

parameters of FVD are derived by directly evaluating the system-level fragility curves of the cable-stayed bridge equipped with these given FVD.

A case study bridge, Polonggou cable-stayed bridge, retrofit with varied FVD is employed to exemplify the methodology. Details of the numerical modeling include nonlinear analysis, the uncertainty treatment, limit state capacities, contribution of critical components to the bridge performance as a system, and so on. For illustration purposes, component fragility curves are developed, which indicate that retrofit measures alters the relative vulnerability of the different components. The system-level fragility curves as well as component fragility curves are compared before and after the application of FVD with different parameters. The results indicate that a given parameter of the FVD may have a positive impact on some components, yet lead to a worse performance of the bridge as a system. Thus, in order to obtain comprehensive insight of bridge performance and derive the accurate optimal parameters of FVD, it is necessary to consider the fragility based on bridge system. The damper exponent α and coefficient C_D are chosen as 0.3 and 8000, respectively, to achieve the best performance of Polonggou cable-stayed bridge as a system.

This methodology can also be employed to perform the optimization of other mitigation devices, the laminated rubber bearing (LRB) system, friction bearing systems, energy dissipation bearing (EDB), shape memory alloy (SMA), and so on. However, it is time consuming to determine the ideal design parameters when the device has more than two characteristic parameters since the substantial effort for the large number of computations. Future work is to propose an efficient computational framework to determine the best performance for isolation devices with multiparameters.

ORCID iD

Jian Zhong https://orcid.org/0000-0002-5998-250X

References

Aiken ID and Kelly JM (1992) Comparative study of four passive energy dissipation systems. *Bulletin of the New Zealand Society for Earthquake Engineering* 25(3): 175–192.

Ali HM and Abdel-Ghaffar AM (1994) Seismic energy dissipation for cable-stayed bridges using passive devices. *Earthquake Engineering & Structural Dynamics* 23(8): 77–93.

ATC (1985) *Earthquake Damage Evaluation Data for California*. Redwood City, CA: Applied Technology Council (ATC).

Avşar O, Yakut A and Caner A (2011) Analytical fragility curves for ordinary highway bridges in Turkey. *Earthquake Spectra* 27(4): 971–996.

Baker JW and Cornell CA (2005) A vector-valued ground motion intensity measure consisting of spectral acceleration and epsilon. *Earthquake Engineering & Structural Dynamics* 34(10): 1193–1217.

Barnawi WT and Dyke SJ (2014) Seismic fragility relationships of a cable-stayed bridge equipped with response modification systems. *Journal of Bridge Engineering* 19(8): A4013003.

Basoz NI, Kiremidjian AS, King SA, et al. (1999) Statistical analysis of bridge damage data from the 1994 Northridge, CA, earthquake. *Earthquake Spectra* 15(1): 25–54.

Bruneau M (1992) Evaluation of system-reliability methods for cable-stayed bridge design. *Journal of Structural Engineering* 118(4): 1106–1120.

Casciati F, Cimellaro GP and Domaneschi M (2008) Seismic reliability of a cable-stayed bridge retrofitted with hysteretic devices. *Computers & Structures* 86(17–18): 1769–1781.

Choi ES, DesRoches R and Nielson B (2004) Seismic fragility of typical bridges in moderate seismic zones. *Engineering Structures* 26(2): 187–199.

Cornell CA, Jalayer F, Hamburger RO, et al. (2002) Probabilistic basis for 2000 SAC Federal Emergency Management Agency steel moment frame guidelines. *Journal of Structural Engineering* 128(4): 526–533.

FEMA (1997) *FEMA 274, NEHRP Commentary on the Guidelines for the Seismic Rehabilitation of Buildings.* Washington, DC: Federal Emergency Management Agency.

Hwang H, Liu JB and Chiu YH (2001) *Seismic Fragility Analysis of Highway Bridges.* Memphis, TN: The University of Memphis.

Luco N and Cornell CA (2007) Structure-specific scalar intensity measures for near-source and ordinary earthquake ground motions. *Earthquake Spectra* 23(2): 357–392.

McKenna FS and Fenves GL (2010) Nonlinear finite-element analysis software architecture using object composition. *Journal of Computing in Civil Engineering* 24(1): 95–107.

Muthukumar S and DesRoches R (2006) A hertz contact model with non-linear damping for pounding simulation. *Earthquake Engineering & Structural Dynamics* 35(7): 811–828.

Nielson BG (2005) *Analytical fragility curves for highway bridges in moderate seismic zones.* PhD Dissertation, Georgia Institute of Technology, Atlanta, GA.

Nielson BG and DesRoches R (2007) Seismic fragility methodology for highway bridges using a component level approach. *Earthquake Engineering & Structural Dynamics* 36(6): 823–839.

Padgett JE and DesRoches R (2008) Methodology for the development of analytical fragility curves for retrofitted bridges. *Earthquake Engineering & Structural Dynamics* 37(8): 1157–1174.

Padgett JE, Nielson BG and DesRoches R (2008) Selection of optimal intensity measures in probabilistic seismic demand models of highway bridge portfolios. *Earthquake Engineering & Structural Dynamics* 37(5): 711–725.

Pan Y, Agrawal AK and Ghosn M (2007) Seismic fragility of continuous steel highway bridges in New York State. *Journal of Bridge Engineering* 12(6): 689–699.

Pang YT, Wu X, Shen GY, et al. (2014) Seismic fragility analysis of cable-stayed bridges considering different sources of uncertainties. *Journal of Bridge Engineering* 19: 04013015.

Ramanathan KN (2012) *Next Generation Seismic Fragility Curves for California Bridges Incorporating the Evolution in Seismic Design Philosophy.* Atlanta, GA: Georgia Institute of Technology.

Ren W and Obata M (1999) Elastic-plastic seismic behavior of long span cable-stayed bridges. *Journal of Bridge Engineering* 4(3): 194–203.

Shafieezadeh A, Ramanathan K, Padgett JE, et al. (2012) Fractional order intensity measures for probabilistic seismic demand modeling applied to highway bridges. *Earthquake Engineering & Structural Dynamics* 41(3): 391–409.

Sharabash AM and Andrawes BO (2009) Application of shape memory alloy dampers in the seismic control of cable-stayed bridges. *Engineering Structures* 31(2): 607–616.

Shinozuka M, Feng MQ, Kim HK, et al. (2000a) Nonlinear static procedure for fragility curve development. *Journal of Engineering Mechanics* 126(12): 1287–1295.

Shinozuka M, Feng MQ, Lee J, et al. (2000b) Statistical analysis of fragility curves. *Journal of Engineering Mechanics* 126(12): 1224–1231.

Wilson JC and Gravelle W (1991) Modeling of a cable-stayed bridge for dynamic analysis. *Earthquake Engineering & Structural Dynamics* 20(8): 707–721.

Zhang J and Huo YL (2009) Evaluating effectiveness and optimum design of isolation devices for highway bridges using the fragility function method. *Engineering Structures* 31(8): 1648–1660.

Zhang Y, Hu X and Zhu S (2009) Seismic performance of benchmark base-isolated bridges with superelastic Cu-Al-Be wire damper. *Structural Control and Health Monitoring* 16(6): 668–685.

Zhong J, Jeon J, Pang Y, et al. (2016) Seismic fragility assessment of long-span cable-stayed bridges in China. *Advances in Structural Engineering* 19(11): 1797–1812.

Zhong J, Jeon JS, Yuan W, et al. (2017) Impact of spatial variability parameters on seismic fragilities of a cable-stayed bridge subjected to differential support motions. *Journal of Bridge Engineering* 22(6): 04017013.

Zhu S and Qiu CX (2014) Incremental dynamic analysis of highway bridges with novel shape memory alloy isolators. *Advances in Structural Engineering* 17(3): 429–438.